

# ErbB4 Modulates Tubular Cell Polarity and Lumen Diameter during Kidney Development

Ville Veikkolainen,<sup>\*,†</sup> Florence Naillat,<sup>‡</sup> Antti Railo,<sup>‡</sup> Lijun Chi,<sup>‡</sup> Aki Manninen,<sup>‡</sup> Peter Hohenstein,<sup>§</sup> Nick Hastie,<sup>§</sup> Seppo Vainio,<sup>‡</sup> and Klaus Elenius<sup>\*,||</sup>

<sup>\*</sup>Department of Medical Biochemistry and Genetics and MediCity Research Laboratory, University of Turku, Turku, Finland; <sup>†</sup>Turku Graduate School of Biomedical Sciences, Turku, Finland; <sup>‡</sup>Oulu Centre for Cell-Matrix Research, Biocenter Oulu, Laboratory of Developmental Biology and Department of Medical Biochemistry and Molecular Biology, University of Oulu, Oulu, Finland; <sup>§</sup>MRC Human Genetics Unit, Western General Hospital, Edinburgh, United Kingdom; and <sup>||</sup>Department of Oncology, Turku University Hospital, Turku, Finland

## ABSTRACT

ErbB4 receptor tyrosine kinase contributes to the development of the heart, the central nervous system, and the lactating mammary gland, but whether it has a role in the development of the kidney epithelium is unknown. Here, we found that expression of *ErbB4* isoforms *JM-a CYT-1* and *JM-a CYT-2* was first detectable around embryonic day 13 in the mouse, mainly in the collecting ducts and both the proximal and distal tubules. *In vitro*, overexpression of a relevant ErbB4 isoform promoted proliferation and disturbed polarization of kidney epithelial cells when cultured as three-dimensional structures. We examined ErbB4 function in developing kidney tubules *in vivo* with *Pax8-Cre*-mediated conditional overexpression of *Rosa26* locus-targeted *ERBB4* and with conditional *ErbB4* knock-out mice. The *Pax8-Cre*-driven *ERBB4* overexpression enhanced proliferation in the collecting ducts, reduced the size of epithelial duct lumens, and promoted formation of cortical tubular cysts. These defects were associated with changes in the subcellular distribution of markers of epithelial cell polarity. Similarly, the *Pax8-Cre*-mediated *ErbB4* knock-out mice manifested dysfunctional kidneys with larger duct lumens and epithelial cell mispolarization. Taken together, these data suggest that ErbB4 signaling modulates proliferation and polarization, cellular functions critical for the development of epithelial ducts in the kidney.

*J Am Soc Nephrol* 23: 112–122, 2012. doi: 10.1681/ASN.2011020160

ErbB4 is a member of the EGF receptor (EGFR) subfamily of receptor tyrosine kinases, which also includes EGFR (ErbB1), ErbB2, and ErbB3.<sup>1</sup> Gene targeting studies have revealed critical roles for ErbB4 in embryogenesis. *ErbB4*-null mice die by embryonic day 11 (E11) as a consequence of defective heart development.<sup>2</sup> The embryonic lethality of *ErbB4*<sup>-/-</sup> mice can be rescued by ectopic expression of human *ERBB4* under an  $\alpha$ -myosin heavy-chain promoter revealing additional functions for ErbB4 in the lactating mammary gland and the central nervous system.<sup>3</sup> There are also indications for a role in kidney development. ErbB4 is expressed in the developing tubules of the nephrons *in vivo*,<sup>4</sup> and overexpression of a relevant ErbB4 isoform in Madin–Darby canine kidney (MDCK) cells promotes tubulogenesis *in vitro*.<sup>5</sup> ErbB4 expression is also downregulated in human renal cell carcinoma<sup>6</sup>

and is upregulated in a mouse model of autosomal recessive polycystic kidney disease.<sup>7</sup>

In this study we addressed the potential role of ErbB4 in mammalian kidney development. We demonstrate that expression of specific *ErbB4* isoforms is induced and maintained in the epithelial segments of the kidney, the nephrons, and the

Received February 15, 2011. Accepted August 17, 2011.

V.V. and F.N. contributed equally to this work.

Published online ahead of print. Publication date available at [www.jasn.org](http://www.jasn.org).

**Correspondence:** Dr. Klaus Elenius, Department of Medical Biochemistry and Genetics, University of Turku, Kiinamyllynkatu 10, FIN-20520 Turku, Finland. Email: [klaus.elenius@utu.fi](mailto:klaus.elenius@utu.fi)

Copyright © 2012 by the American Society of Nephrology

collecting ducts. *ErbB4* gain- and loss-of-function studies in kidney epithelial cells *in vitro* and *in vivo* demonstrated altered ductal epithelial cell proliferation and compromised expression of proteins that are normally expressed in a polarized manner in the ducts. These results are in line with a conclusion that ErbB4 signaling is involved in the control of proliferation and polarization of kidney epithelial cells in the nephrons and collecting ducts during kidney development.

## RESULTS

### Developing Nephrons and Ureteric Epithelium Selectively Express Cleavable *ErbB4* JM-a Isoforms

The *ErbB4* gene is expressed as four alternatively spliced isoforms with unique signaling characteristics.<sup>8,9</sup> The isoforms are composed of alternative extracellular juxtamembrane (JM) and intracellular cytoplasmic (CYT) domains (Figure 1A). The expression of all four *ErbB4* isoforms in the kidneys of CD-1 mice was analyzed at developmental stages E10.5 through P0 (newborn) by real-time reverse transcriptase (RT)-PCR (Figure 1B). *ErbB4* expression was detected from E12.5 onward, and the expression level increased until birth. Only isoforms JM-a CYT-1 and JM-a CYT-2 were present, and JM-a CYT-2 was more abundant. The gene encoding the ErbB4 ligand *Nrg-1* was expressed throughout kidney development (Figure 1B). In addition to *ErbB4*, *Egfr*, *ErbB2*, and *ErbB3* were also expressed in varying concentrations (maximally 1.2%, 19.3%, and 1.0% of  $\beta$ -actin mRNA, respectively), indicating that ErbB4 may signal in the developing kidney both as a homodimer and as a heterodimer.

To define the cells that express *ErbB4*, *in situ* hybridization and anti-ErbB4 immunohistochemistry were carried out. In accordance with the real-time RT-PCR data (Figure 1B), *ErbB4* expression was detected in epithelial cells at E14.5 (Figure 1C). At later stages of nephrogenesis, the expression was confined to their derivatives, the proximal and distal tubules and the loops of Henle. In addition to the developing nephrons, *ErbB4* was expressed in ureteric bud-derived collecting duct epithelium in the medulla and in the papillae (Figure 1, D and E). Tissue recombination experiments with separated E11.5 kidney mesenchymes and a heterologous inducer tissue indicated that *ErbB4* was activated in epithelializing pretubular aggregates in the induced mesenchyme (Figure 1F). *ErbB4* expression was very low in uninduced kidney mesenchyme but was activated in epithelializing mesenchymal cells after 48 hours of tubule induction (Figure 1G). The expression was further upregulated at 96 and 120 hours in culture, indicating that *ErbB4* expression is not activated as an immediate early response to tubule induction but is associated with epithelialization of the mesenchymal cells.

Only the *ErbB4* JM-a isoforms can be proteolytically cleaved to produce a soluble intracellular domain that can translocate into the nucleus and regulate transcription.<sup>10–12</sup> Indeed, both nuclear and cell membrane immunostaining for

ErbB4 was observed in the developing tubules (Figure 1H). Taken together, these findings demonstrate that cleavable *ErbB4* isoforms are expressed during kidney ontogeny by the epithelia of the maturing nephrons and the collecting ducts.

### ERBB4 Gain-of-Function Disrupts Polarization and Cyst Formation of Tubular Epithelial Cells *In Vitro*

Kidney-derived MDCK epithelial cells were used to address the effects of ErbB4 signaling on kidney epithelium at the cellular level. When cultured in three-dimensional matrices, MDCK cells form cysts, *i.e.*, hollow spheres lined by epithelium, and can be used as a model system to study such events as epithelial morphogenesis, cell polarization, and lumen formation.<sup>13,14</sup> The MDCK cells were infected with retroviral constructs encoding *ERBB4* JM-a CYT-2 or an empty vector control (Figure 2A), cultured for 5 days in Matrigel (BD Biosciences), and monitored for proliferation and cyst formation (Figure 2, B–E). MDCK cysts overexpressing *ERBB4* contained significantly ( $P < 0.001$ ) more Ki-67–positive proliferating cells compared with control cysts (Figure 2, B and C). Unexpectedly, cells overexpressing *ERBB4* also exhibited abnormal cyst polarization as they formed significantly ( $P = 0.008$ ) more cysts composed of multiple lumens compared with control cells; a majority of the latter formed cysts with a single lumen (Figure 2, D and E).

These findings indicate that ErbB4 controls kidney epithelial cell proliferation, polarization, and cyst formation *in vitro*.

### ERBB4 Gain-of-Function Enhances Proliferation of Collecting-Duct Epithelial Cells, Interferes with the Development of Proximal Tubules, and Promotes Cyst Formation during Kidney Organogenesis *In Vivo*

To address the effect of *ERBB4* gain-of-function on kidney development *in vivo*, a construct with human *ERBB4* JM-a CYT-2 cDNA under a floxed transcriptional stop cassette was inserted into the genomic *Rosa26* locus to generate *R26ERBB4* mice (Supplemental Figure 1, A and B). The cleavable *ERBB4* JM-a CYT-2 isoform was chosen because it was the prevailing isoform expressed in the kidney (Figure 1B). The *Pax8-Cre* mouse line was used to activate *ERBB4* expression in the developing kidney. Cre recombinase under the control of the *Pax8* promoter (*Pax8-Cre*) recombines a floxed reporter gene in the ureteric epithelial cells and the nephron-forming mesenchymal cells after their aggregation from around E11.5 onward (Supplemental Figure 1C).<sup>15</sup> Crossing the *Pax8-Cre* line with the *R26ERBB4* line led to the expected gain-of-function expression of human ErbB4 protein in the relevant epithelial structures in the developing kidneys of the *R26ERBB4/Pax8-Cre* embryos (Supplemental Figure 2, A–D). Analysis of ErbB4-activated signaling demonstrated enhanced ErbB4 and Erk phosphorylation in the mutant mice, while no significant effect on Akt phosphorylation was detected (Supplemental Figure 2, C–E).

Histologic examination of newborn *R26ERBB4*<sup>+/–</sup>/*Pax8-Cre*<sup>+</sup> mouse kidneys revealed characteristic phenotypes in

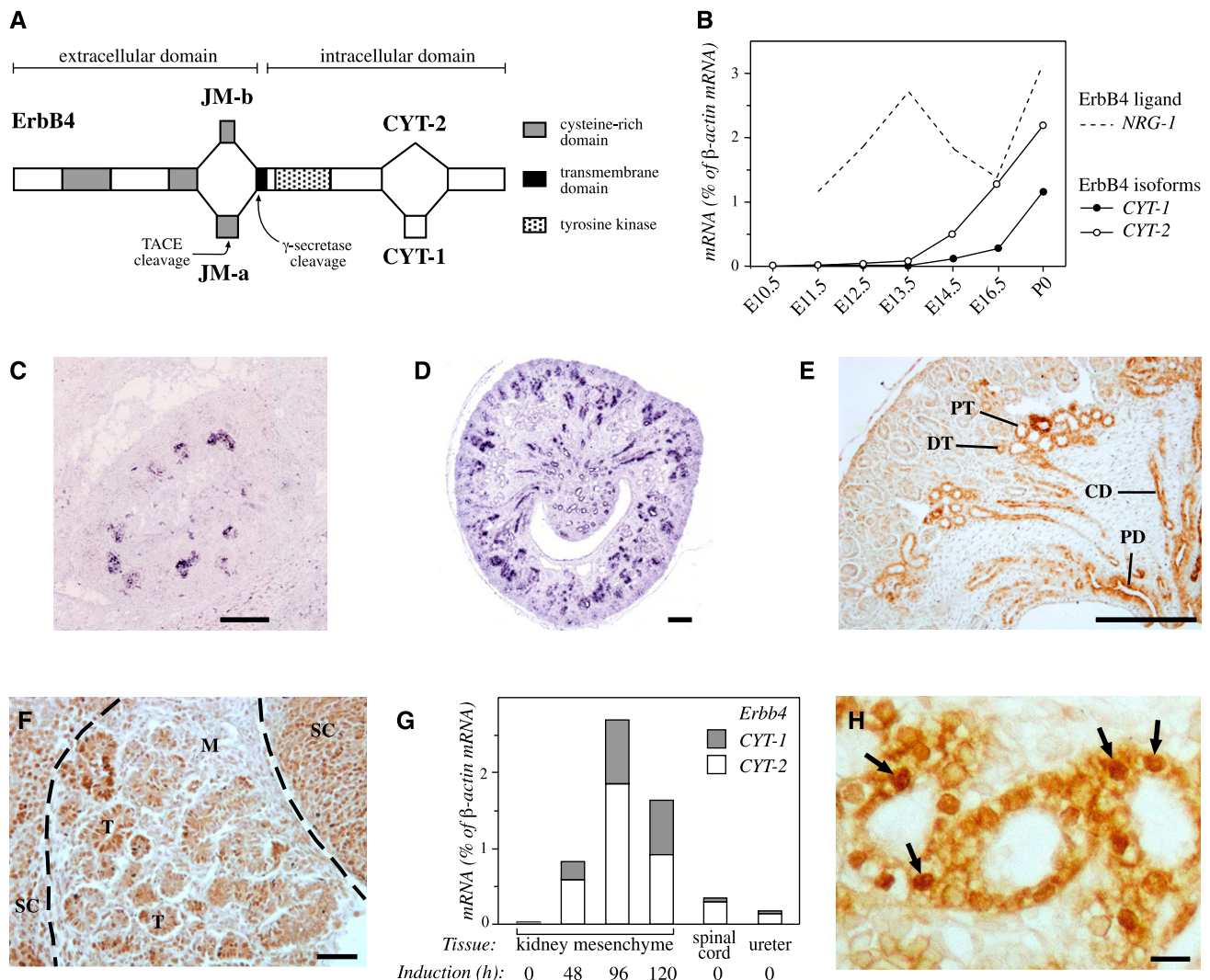


**Figure 1.** *ErbB4* expression during kidney development. (A) Four *ErbB4* isoforms are generated by alternative splicing. The isoforms differ at the extracellular JM or the CYT domains. JM-a isoforms can be cleaved by the tumor necrosis factor- $\alpha$ -converting enzyme (TACE) and  $\gamma$ -secretase to produce a soluble intracellular domain capable of translocating to the nucleus and regulating transcription.<sup>10,11,49</sup> CYT-2 isoforms differ from CYT-1 isoforms by lacking 16 amino acids known to include a PI3-K binding site and a proline-rich interaction motif for WW domain-containing proteins.<sup>9,43</sup> (B) Expression of transcripts encoding all four *ErbB4* isoforms and the *ErbB4* ligand *Nrg-1* were analyzed at different stages of mouse kidney development by real-time RT-PCR. Only isoforms JM-a CYT-1 and JM-a CYT-2 were detected.  $\beta$ -actin was used as a reference gene to normalize expression levels. (C and D) *In situ* hybridization analysis of *ErbB4* in E14.5 (C) and E17.5 (D) mouse kidneys demonstrated expression in the developing collecting ducts, adjacent epithelializing kidney mesenchymal cells, and relatively well-differentiated nephrons in the medulla. Alkaline phosphatase chromogen 5-bromo-4-chloro-3-indolyl-phosphatase/nitro blue tetrazolium (BCIP/NBT) (Roche Applied Science, Penzberg, Germany) was used to detect the probe. (E) Immunohistochemical analysis of *ErbB4* expression in E16.5 mouse kidney demonstrated expression in developing epithelial structures consistent with the *in situ* hybridization analysis. CD, collecting duct; DT, distal tubule; PD, papillary duct; PT, proximal tubule. (F) Immunohistochemical analysis of *ErbB4* expression in kidney mesenchyme induced for 84 hours with spinal cord demonstrated expression in induced epithelial structures. M, mesenchyme; SC, spinal cord; T, tubules developing from renal vesicles. (G) Real-time RT-PCR analysis of *ErbB4* JM-a CYT-1 and JM-a CYT-2 isoform expression in uninduced mesenchyme; cultured mesenchyme induced with spinal cord for 48, 96, and 120 hours; spinal cord; and ureter.  $\beta$ -actin was used as a reference gene to normalize expression levels. (H) Immunohistochemical analysis of E16.5 mouse kidney with an antibody (sc-283) recognizing the carboxy-terminus of *ErbB4* demonstrated nuclear immunoreactivity in proximal tubule cells (arrows). (E, F, and H) The 3,3'-diaminobenzidine (DAB) peroxidase substrate kit was used to detect the antibodies (Vector Laboratories, Burlingame, CA). Scale bars: (C and D) 250  $\mu$ m; (E) 200  $\mu$ m; (F) 50  $\mu$ m; (H) 10  $\mu$ m.

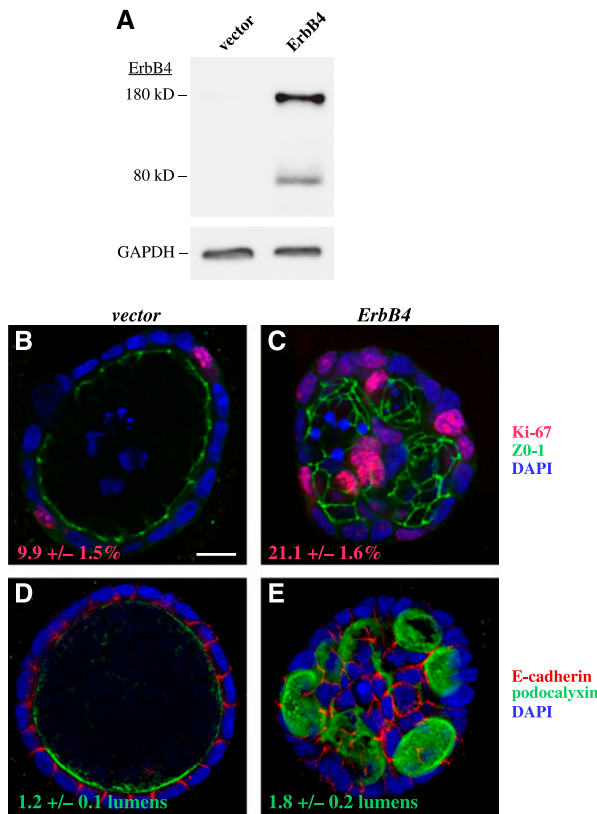


**Figure 2.** *ERBB4* overexpression promotes proliferation and disrupts polarization of epithelial cells *in vitro*. (A) Western analysis of ErbB4 expression in MDCK cells infected with a retrovirus encoding the *ERBB4* JM-a CYT-2 isoform or an empty vector control. Glyceraldehyde 3-phosphate dehydrogenase (GAPDH) was analyzed as a loading control. (B and C) MDCK cells were cultured in Matrigel for 5 days and stained for Ki-67 (red), ZO-1 (green), and 4',6-diamidino-2-phenylindole (DAPI) (blue), to visualize proliferating cells, tight junctions, and nuclei, respectively. Cysts formed by cells overexpressing *ERBB4* contained significantly more proliferating cells compared with vector control cysts ( $P < 0.001$ ). The percentage of Ki-67-positive cells out of DAPI-stained cells  $\pm$  SEM is indicated. Scale bar: (B) 10  $\mu$ m. (D and E) MDCK cysts were stained for E-cadherin (red), podocalyxin (green), and DAPI (blue) to visualize basolateral and apical surfaces and nuclei, respectively. Cysts formed by cells overexpressing *ERBB4* formed significantly more lumens compared with the vector control cysts ( $P = 0.008$ ). The number of lumens per cyst  $\pm$  SEM is indicated.

the medulla and the cortex (Figure 3, A and B). Compared with the wild-type kidney, the mutant medulla had an irregular structure with clearly defective collecting duct organization (Figure 3, D and E). Morphometric measurements demonstrated that the cell density in the medullae of the mutant mice was significantly increased compared with wild-type kidneys (Figure 3C). In addition, the average diameter of the collecting duct lumen was significantly reduced (Figure 3F). As ErbB4 activation increased proliferation of kidney epithelial cells *in vitro* (Figure 2, B and C), newborn *R26ERBB4/Pax8-Cre* kidneys were analyzed with proliferating cell nuclear

antigen (PCNA) immunostaining (Figure 3, G and H). Indeed, mutant papillary epithelial cells included a significantly greater percentage of PCNA-positive cells compared with wild-type samples (Figure 3I).

Defects were also observed in the mutant cortices, in particular in the proximal tubules, the epithelial structures most abundantly expressing endogenous ErbB4 (Figure 1, E and H). The proximal tubules of the mutant mice frequently demonstrated abnormal structure with lost or reduced lumens (Figure 4, A and B). In addition, *in situ* hybridization analysis with the proximal tubule marker *Slc3A1* indicated a reduced number of proximal tubules in mutant mice (Figure 4, C and D). The structure of the distal tubules, however, was not affected by *ERBB4* gain-of-function (Figure 4, E and F). Of note, abnormal formation of cortical tubular cysts was observed in approximately 50% of the kidneys of newborn mutant mice (Figure 4G). Immunohistochemical analysis demonstrated enhanced ErbB4 expression in the epithelial lining of the cysts but also showed that the expression was gradually lost when the diameter of the cysts increased (data not shown).

#### ***ERBB4* Gain-of-Function Disrupts Polarization and Lumen Formation in Collecting Ducts and Proximal Tubules *In Vivo***

To address whether the observed phenotypes associated with defects in epithelial cell polarization, sections representing *R26ERBB4/Pax8-Cre* newborn kidneys were immunostained for aquaporin-1, aquaporin-2,<sup>16</sup> *Dolichos bifloris* agglutinin (DBA),<sup>17</sup> acetylated  $\alpha$ -tubulin,<sup>18</sup> and thiazide-sensitive NaCl cotransporter.<sup>19</sup>

Normally the collecting duct epithelium is composed of a single layer of cuboidal cells that are well lined next to each other (Figure 5, A and C). The *ERBB4* gain-of-function changed this organization, and many of the ductal cells were morphologically abnormal and irregularly organized within the epithelial cell layer (Figure 5, B and D). Aquaporin-2 expression in the wild-type collecting ducts was polarized to the apical membranes of the epithelial cells (Figure 5A). In contrast, *ERBB4* gain-of-function changed this pattern, and aquaporin-2 became localized into intracellular vesicles dispersed throughout the cytosol of epithelial cells (Figure 5B). Polarization of another collecting duct marker, DBA, was also altered, and its localization became restricted to apical surfaces in the mutant mice, whereas both apical and basolateral expression was seen in wild-type mice (Figure 5, C and D). *ERBB4* gain-of-function also reduced the expression levels of DBA. Moreover, polarization of the tight-junction marker ZO-1 to the lateral membranes of the collecting-duct epithelial cells was partially disrupted in response to *ERBB4* gain-of-function (data not shown). Immunostaining for acetylated  $\alpha$ -tubulin, in turn, indicated that the primary cilia of the mutant collecting ducts were not dramatically affected (Figure 5, E and F).

One characteristic feature of a developing duct is the regulation of the orientation of cell division. Division along



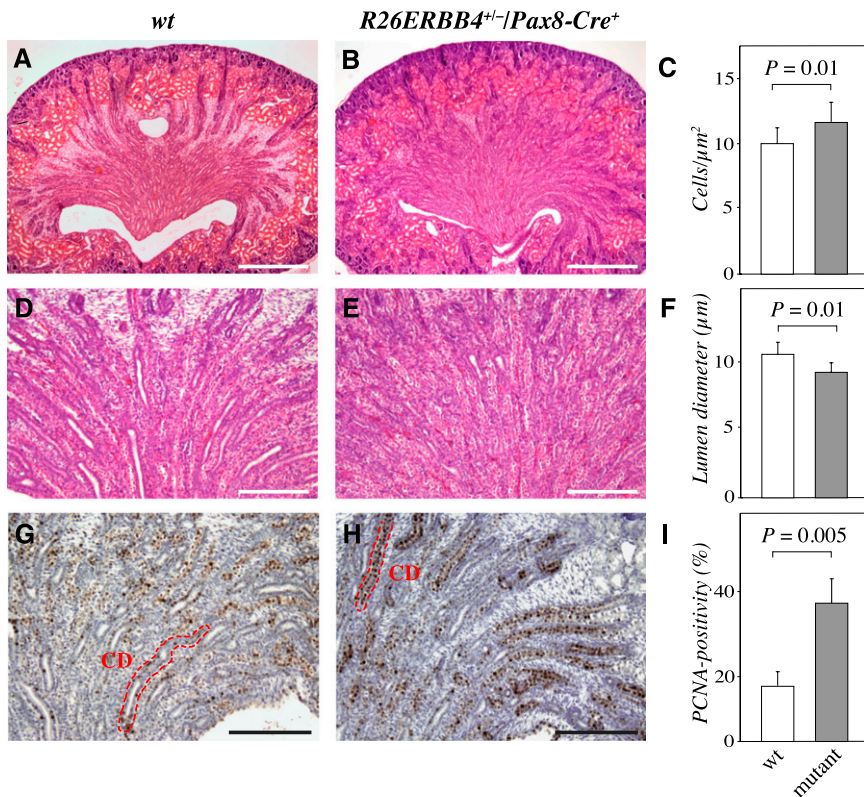


**Figure 3.** *ERBB4* gain-of-function leads to defective collecting duct development. Paraffin sections of *R26ERBB4/Pax8-Cre* kidneys (newborn) were stained with hematoxylin and eosin (A, B, D, and E) or with anti-PCNA and hematoxylin (G and H). *R26ERBB4<sup>+/-</sup>/Pax8-Cre<sup>+</sup>* mutant mice demonstrated enhanced cellular density in the medulla (A–C), reduced mean diameter of collecting duct lumen (D–F), and increased amount of PCNA-positive tubular epithelial cells (dark brown signals) indicating enhanced proliferation (G–I). CD, collecting duct; wt, *R26ERBB4<sup>+/-</sup>/Pax8-Cre<sup>-</sup>*. Scale bars: (A and B) 500  $\mu\text{m}$ ; (D and E) 200  $\mu\text{m}$ ; (G and H) 250  $\mu\text{m}$ .

the longitudinal axis of the duct increases the length of the duct, and radial division dilates the duct.<sup>20,21</sup> To address whether the observed changes in the lumen size (Figures 3F and 4, A and B), proliferation (Figure 3I), and polarity (Figure 5, A–D) of the collecting duct epithelia were associated with changes in the axis of epithelial cell division, sections of *R26ERBB4/Pax8-Cre* newborn kidneys were immunostained with antibodies recognizing phosphorylated histone H3, and the axis of mitosis in relation to the axis of the lumen of the duct was determined under the microscope.<sup>21</sup> Indeed, *ERBB4* overexpression significantly increased the percentage of dividing collecting duct epithelial cells demonstrating radial axis of mitosis, compared with the control mice, which mostly demonstrated longitudinal cell division (Figure 5, G–I).

Similar to aquaporin-2 localization in the collecting ducts, aquaporin-1 in the mutant proximal tubule epithelia was localized throughout the cytosol as opposed to the apical cell surface polarization observed in the wild-type controls (Figure 6, A and B). The polarization of NaCl cotransporter in the mutant distal tubules, in contrast, appeared undisturbed and

similar to that of wild-type tissues (Figure 6, C and D). These findings about the tubular cell polarization are consistent with the defects in the structure of the proximal (Figure 4, A and B) but not distal (Figure 4, E and F) tubule cells.

Taken together, these data suggest that *ERBB4* gain-of-function in the developing kidney epithelium leads to defective polarization in collecting duct and proximal tubule epithelium, as well as to changes in the axis of cell division in the developing collecting duct.

### *ErbB4* Loss-of-Function Disrupts Polarization and Lumen Formation in Collecting Ducts and Proximal Tubules In Vivo

To further address the role of *ErbB4* in regulating kidney tubulogenesis, *ErbB4* signaling was conditionally inactivated using Cre recombinase under the *Pax8* promoter to generate *ErbB4<sup>Flox/Flox</sup>/Pax8-Cre<sup>+</sup>* mice. The *ErbB4<sup>Flox/Flox</sup>/Pax8-Cre<sup>+</sup>* genotype was over-represented in prematurely terminated resorbed embryos at E11.5–E16.5 (8 mutants out of a total of 12 dead embryos;  $P < 0.001$ ). Moreover, at birth, significantly fewer viable pups had the *ErbB4<sup>Flox/Flox</sup>/Pax8-Cre<sup>+</sup>* genotype (12.9%) than expected (25%) from the normal Mendelian distribution ( $P = 0.02$ ) (Table 1). Because *Pax8* expression is also detectable in the developing heart<sup>22</sup> and the *ErbB4* null mice die by E11 with defective heart development,<sup>2</sup> it is possible that heart-specific effects contributed to the compromised viability of the *ErbB4<sup>Flox/Flox</sup>/Pax8-Cre<sup>+</sup>* mice.

To minimize the contribution of possible developmental heart defects and subsequent changes in tissue perfusion on kidney development and function, the born mutant mice were not examined until adulthood (4 months of age). Four-month-old mutant mice did not exhibit signs of heart failure, such as edema at autopsy, and the lack of hypoxia in the mutant kidneys was documented by immunohistochemical analysis of hypoxia-inducible factor-1 $\alpha$  expression (data not shown).

The kidneys of the surviving *ErbB4<sup>Flox/Flox</sup>/Pax8-Cre<sup>+</sup>* mice demonstrated significantly reduced or lost *ErbB4* expression (Supplemental Figure 3, A–E), and no signal for phosphorylated *ErbB4* was detected (Supplemental Figure 3E). Analysis of Erk and Akt downstream signaling pathways indicated modestly reduced Akt phosphorylation in response to *ErbB4* loss-of-function (Supplemental Figure 3E).

The mutant mice demonstrated abnormal kidney histologic features, with significantly more fibrotic tissue surrounding the Bowman capsules compared with wild-type kidneys (Figure 7,

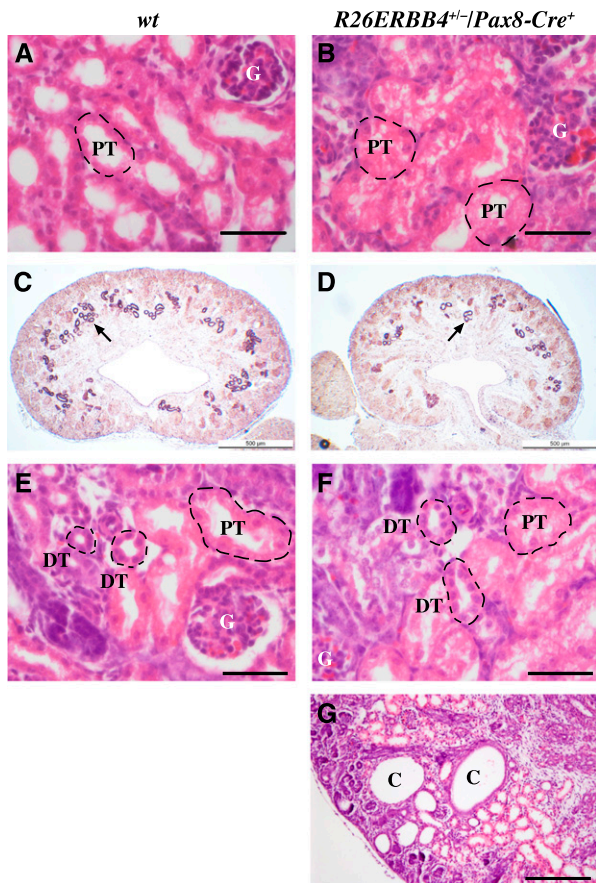


**Figure 4.** *ERBB4* gain-of-function results in defective proximal tubule development and leads to cyst formation. Paraffin sections of *R26ERBB4/Pax8-Cre* kidneys were stained with hematoxylin and eosin (A, B, E, F, and G) or analyzed by *in situ* hybridization to detect expression of the proximal tubule marker *Slc3A1* (C and D). *R26ERBB4<sup>+/</sup>/Pax8-Cre<sup>+</sup>* mutant mice demonstrated aberrant proximal tubule structure with reduced luminal space (P0) (A and B) and a reduced number of proximal tubules, as indicated by *Slc3A1* expression (purple indicated by arrow; E16.5) (C and D). The distal tubules, however, appeared normal (P0) (E and F). Tubular cysts were observed in kidneys of mutant mice (P0) (G). C, cyst; DT, distal tubule; G, glomerulus; PT, proximal tubule; wt, *R26ERBB4<sup>-/-</sup>/Pax8-Cre<sup>-</sup>*. Scale bars: (A, B, E, and F) 50  $\mu$ m; (C and D) 500  $\mu$ m; (G) 200  $\mu$ m.

A, B, and E). Consistent with the gain-of-function data that indicated increased cell density as a result of *ERBB4* over-expression, the density of cells in the medullae of the *ErbB4* loss-of-function mice was significantly reduced (Figure 7F). Furthermore, the surviving mice manifested significantly dilated collecting ducts (Figure 7, C, D, and G).

Immunohistochemical analyses of the *ErbB4* loss-of-function mice with antibodies recognizing aquaporin-2 and DBA indicated mispolarization of the collecting duct epithelial cells (Figure 8, A–D). Similarly, analyses with antibodies recognizing aquaporin-1 and another proximal tubule marker, *Lotus tetragonolobus* lectin, indicated mispolarization

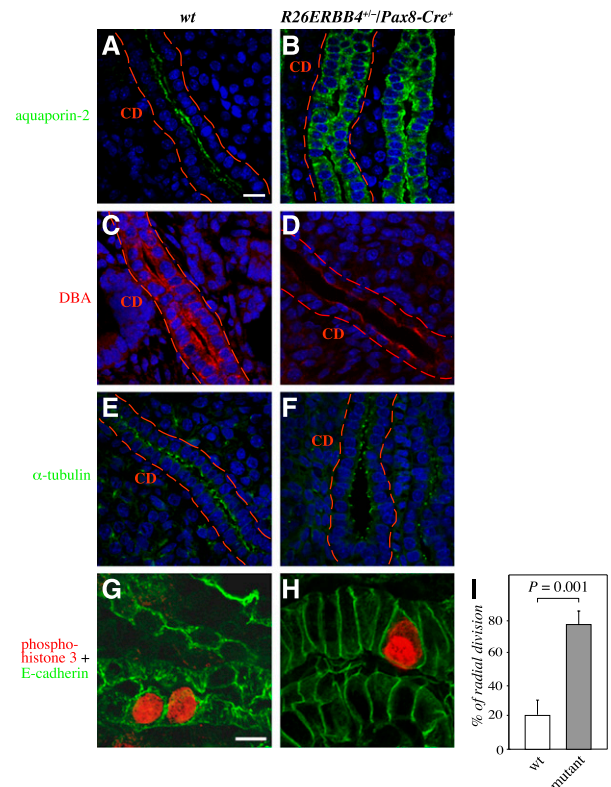


**Figure 5.** *ERBB4* gain-of-function disrupts polarization and enhances radial cell division of collecting-duct epithelial cells. (A–H) Immunohistochemical analyses of *R26ERBB4/Pax8-Cre* kidneys (P0) visualized by confocal microscopy. Staining for aquaporin-2 (green) and DBA (red) demonstrated altered polarization and disorganization of *R26ERBB4<sup>+/</sup>/Pax8-Cre<sup>+</sup>* mutant collecting duct epithelium (A–D). Expression of  $\alpha$ -tubulin (green), in epithelial cell cilia of mutant collecting ducts was not significantly altered (E and F). The sections were stained for phospho-histone H3 (red) to define the axis of mitoses and with E-cadherin (green) to visualize cell borders (G and H). When the orientation of mitosis in collecting ducts was scored as longitudinal or radial (non-axis parallel) divisions, the mutant mice demonstrated significantly more radial cell divisions compared with the wild-type controls (I). Nuclei were stained with DAPI (blue). CD, collecting duct; wt, *R26ERBB4<sup>-/-</sup>/Pax8-Cre<sup>-</sup>*. Scale bars: (A) 20  $\mu$ m; (G) 10  $\mu$ m.

of epithelial cells in the proximal tubules (Figure 8, E–H). These data indicate that, consistent with the observations based on the Pax8-Cre-mediated gain-of-function, the Pax8-Cre-mediated loss-of-function of *ErbB4* leads to defective control of tubular epithelial cell growth and polarization.

## DISCUSSION

The *ERBB4* gene is actively expressed in the mature functional kidney.<sup>4,23</sup> Previous *in vitro* work has demonstrated that the cleavable ErbB4 JM-a CYT-2 isoform promotes tubule formation in kidney epithelial cells.<sup>5</sup> According to our real-time



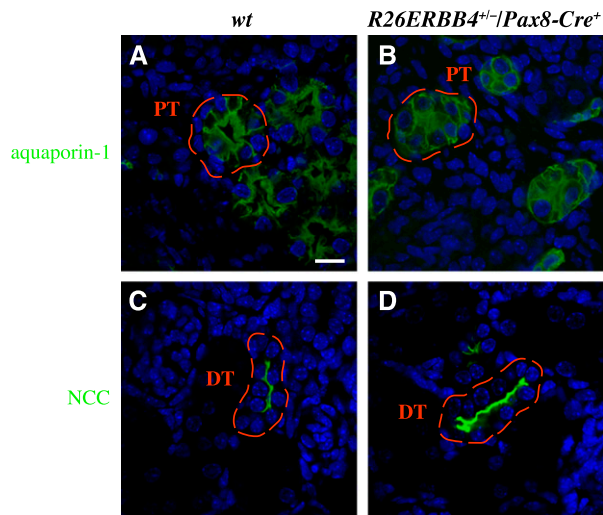


**Figure 6.** *ERBB4* gain-of-function disrupts polarization of proximal tubule epithelial cells. (A–D) Immunohistochemical analyses of *R26ERBB4*<sup>+/</sup>/*Pax8-Cre*<sup>+</sup> kidneys (P0) visualized by confocal microscopy. Aquaporin-1 staining (green) demonstrated altered polarization and reduced lumen size of mutant proximal tubule epithelium (A and B). NaCl cotransporter (NCC) staining (green) indicated normal polarization and structure of mutant distal tubule epithelial cells (C and D). Nuclei were stained with DAPI (blue). DT, distal tubule; PT, proximal tubule; wt, *R26ERBB4*<sup>+/</sup>/*Pax8-Cre*<sup>+</sup>. Scale bar: (A) 20  $\mu$ m.

**Table 1.** Genotype distribution of *Erb4*<sup>Flox</sup>/*Pax8-Cre* mice in different developmental stages

Stage	Mice Alive/Dead (n/n)				Total
	FF Cre <sup>+</sup>	F <sup>+</sup> Cre <sup>+</sup>	FF Cre <sup>-</sup>	F <sup>+</sup> Cre <sup>-</sup>	
E11.5	12/5	16/0	21/1	15/0	64/6
E12.5	3/1	6/0	2/1	4/0	15/2
E16.5	5/2	6/0	7/0	2/1	20/3
P0	9/0	23/0	25/0	13/1	70/1
All	29/8	51/0	55/2	34/2	169/12

*Erb4*<sup>Flox/Flox</sup> mice were bred with *Erb4*<sup>Flox/+</sup>/*Pax8-Cre*<sup>+</sup> mice. Heterozygous *Pax8-Cre*-mediated *Erb4* knock-out resulted in fewer live pups at birth (P0) compared with expected (25%) Mendelian distribution ( $P=0.02$ ). Significantly more dead *Erb4*<sup>Flox/Flox</sup>/*Pax8-Cre*<sup>+</sup> embryos were also observed (E11.5–P0) compared with other genotypes ( $P<0.001$ ). FF Cre<sup>+</sup>, *Erb4*<sup>Flox/Flox</sup>/*Pax8-Cre*<sup>+</sup>; F<sup>+</sup> Cre<sup>+</sup>, *Erb4*<sup>Flox/+</sup>/*Pax8-Cre*<sup>+</sup>; FF Cre<sup>-</sup>, *Erb4*<sup>Flox/Flox</sup>/*Pax8-Cre*<sup>-</sup>; F<sup>+</sup> Cre<sup>-</sup>, *Erb4*<sup>Flox/+</sup>/*Pax8-Cre*<sup>-</sup>.

RT-PCR, *in situ* hybridization, and immunohistochemical analyses, *Erb4* was also expressed during kidney development *in vivo*. Expression of cleavable *Erb4* isoforms *JM-a* CYT-1 and *JM-a* CYT-2 was activated starting at E12.5 in association with epithelialization of the embryonic kidney mesenchymal cells during nephrogenesis. In addition, *Erb4* was present in the developing ureteric bud that generates the collecting-duct cells and the ureter. The observed *Erb4* expression pattern suggests that this signaling protein has a role in the development of kidney epithelium.

Functional gain-of-function and loss-of-function studies indicated a role for *Erb4* in orchestrating nephrogenic epithelial cell proliferation. Increased epithelial cell proliferation *in vitro*

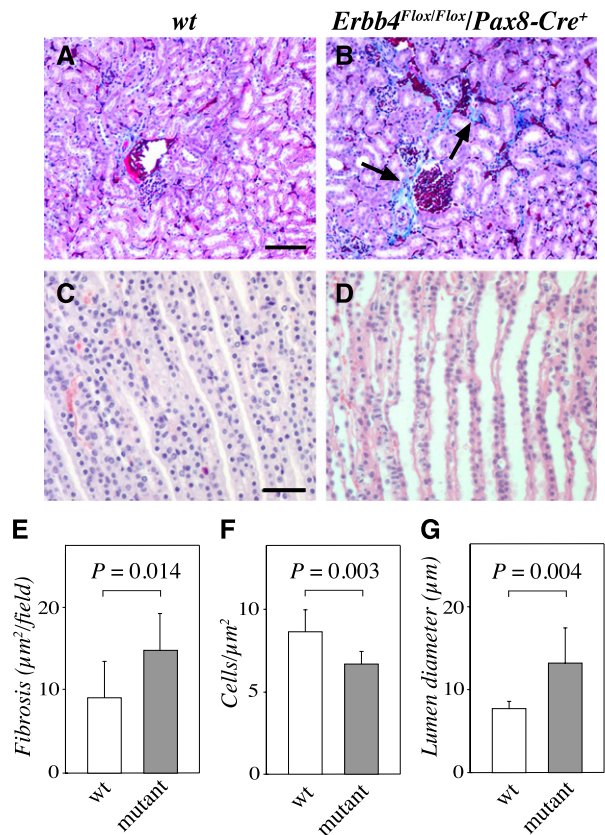


**Figure 7.** *Erb4* loss-of-function reduces medullar cell density and increases collecting duct lumen size. Paraffin sections of *Erb4*<sup>Flox/Flox</sup>/*Pax8-Cre* (adult) kidneys were stained with Masson trichrome staining to visualize fibrosis (A and B) or with hematoxylin and eosin to visualize structure (C and D). Mutant kidneys demonstrated significantly increased fibrosis around the glomeruli (blue color indicated with arrows in B) (A, B, and E), and irregular collecting-duct structure compared with the wild-type controls (C and D). (F and G) Morphometric analyses demonstrated that the cell density in the medulla was reduced (F), whereas the mean diameter of the collecting duct lumens was increased (G) in the kidneys with *Erb4* loss-of-function. wt, *Erb4*<sup>Flox/Flox</sup>/*Pax8-Cre*<sup>-</sup>. Scale bars: (A) 100  $\mu$ m; (C) 50  $\mu$ m.

(by 2.1-fold) was observed in kidney-derived MDCK epithelial cells overexpressing the relevant *ERBB4* isoform, *JM-a* CYT-2. Moreover, transgenic mice with *Pax8* promoter-driven overexpression of *ERBB4* *JM-a* CYT-2 in the developing kidney resulted in significantly increased cell density in the medulla (by 1.14-fold) and in enhanced proliferation (by 2.6-fold) of the epithelial cells of the collecting ducts. Finally, data from mice with conditional *Erb4* loss-of-function under the *Pax8* promoter demonstrated a significant decrease in cell density in the medulla (by 1.3-fold). These findings are in line with previous data suggesting that the cleavable *Erb4* *JM-a* CYT-2 isoform selectively promotes proliferation *in vitro*<sup>11,24</sup> and in the mammary epithelium *in vivo*.<sup>25</sup>

In addition to enhanced proliferation, disturbed epithelial cell polarization was observed in the MDCK cells overexpressing

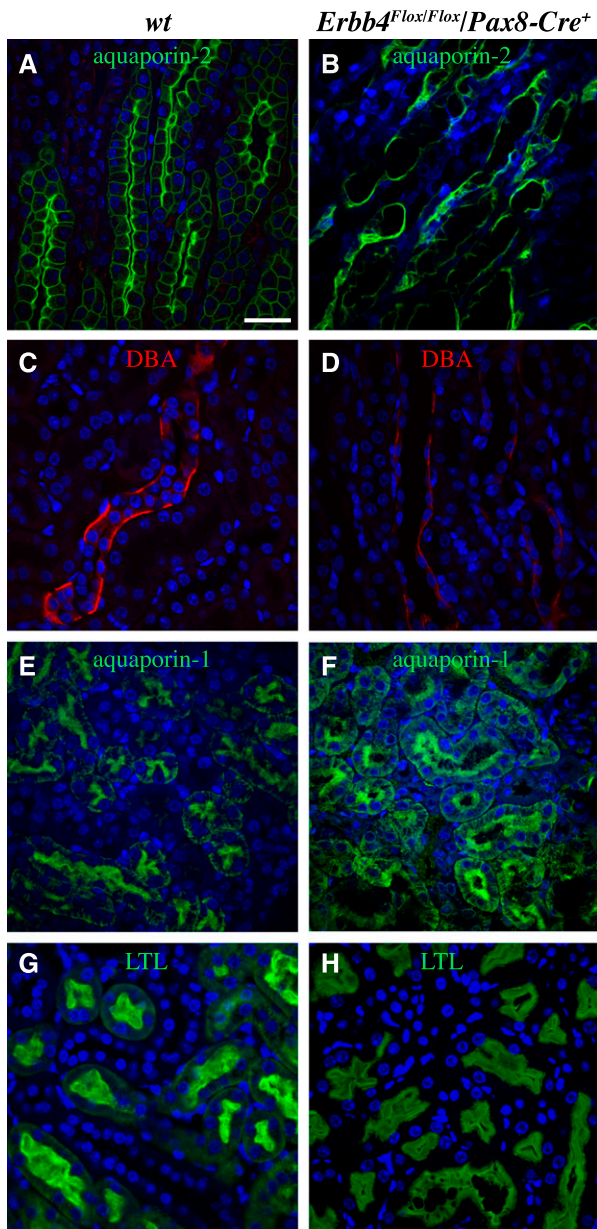


**Figure 8.** *ErbB4* loss-of-function disrupts polarization of tubular epithelial cells. (A–H) Immunohistochemical analyses of *ErbB4*<sup>Flox</sup>/*Pax8-Cre* kidneys (adult) visualized by confocal microscopy. Aquaporin-2 (A and B; green) and DBA (B and C; red) staining demonstrated aberrant structure and polarization of collecting ducts of *ErbB4* knock-out mice. Aquaporin-1 (E and F; green) and *Lotus tetragonolobus* lectin (LTL) (G and H; green) staining demonstrated enlarged lumens and disrupted polarization of proximal tubules of *ErbB4* knock-out mice. Nuclei were stained with DAPI (blue). wt, *ErbB4*<sup>Flox/Flox</sup>/*Pax8-Cre*<sup>−</sup>. Scale bar (A): 50  $\mu$ m.

*ERBB4*, as well as in both gain- and loss-of-function mouse models. Because polarization of one of the used markers, aquaporin-2, has been shown to be regulated by the hydration status of the body,<sup>26</sup> the analyses were also carried out with aquaporin-2-independent markers: DBA, LT-1, aquaporin-1,

and ZO-1. The observation that plasma creatinine and electrolyte concentrations did not significantly differ between the knock-out and wild-type mice (data not shown) also indicated that the hydration status of the mice was similar. Furthermore, *ERBB4* overexpression induced changes in kidney epithelial cell polarization *in vitro*, demonstrating that ErbB4 activity is sufficient to affect polarization under conditions with controlled water balance.

An intriguing finding was that the orientation of epithelial cell proliferation was more radial in relation to the axis of the collecting-duct lumen in mice with *ERBB4* gain-of-function compared with wild-type controls. This finding is consistent with the observed changes in the lumen diameter of the collecting ducts in both the gain- and loss-of-function mouse models because radial orientation of cell division increases the width of the kidney collecting duct epithelium, whereas an increase of cell division along the longitudinal axis increases the length of the duct.<sup>20,21</sup> Of note, misorientation of cell division has also been implicated as having a role in cyst formation in the kidney,<sup>20,27,28</sup> and epithelial cortical cysts were occasionally observed in our model of *ERBB4* gain-of-function. Taken together, these findings indicate that ErbB4 regulates normal kidney development by controlling polarization and orientation of cell division, whereas deregulated ErbB4 signaling may lead to epithelial cystogenesis.

ErbB signaling has also been associated with formation of renal cysts in previous studies. Indeed, an *ERBB4* allele has been reported to be lost in a patient with a polycystic kidney and early myoclonic encephalopathy.<sup>29</sup> In addition, increased ErbB4 expression has been shown in a mouse model of autosomal recessive polycystic kidney disease.<sup>7</sup> Of the other ErbBs, deregulated EGFR and ErbB2 signaling has been associated with human autosomal recessive polycystic kidney disease (PKD),<sup>30,31</sup> autosomal dominant PKD,<sup>32,33</sup> and with rodent models of both forms of PKD.<sup>34,35</sup> Furthermore, ErbB2 inhibition reduces cyst formation in a mouse model of PKD and rescues the impaired migration of epithelial cell lines isolated from patients with autosomal dominant PKD.<sup>34</sup> Thus, several lines of evidence imply a role for ErbB signaling in the generation of renal cysts both in mouse models and in human disease.

In summary, we demonstrate that specific isoforms of the *ErbB4* receptor tyrosine kinase are induced in both mesenchyme- and ureteric bud-derived epithelia of the embryonic kidney. In addition, these findings indicate a functional role for ErbB4 signaling pathway in establishing and maintaining the kidney epithelium by controlling proliferation, polarization, and orientation of cell division.

## CONCISE METHODS

### Animals

*ErbB4*<sup>Flox/Flox</sup>,<sup>36</sup> *Pax8-Cre*,<sup>15,37</sup> and *Rosa26LacZ*<sup>37</sup> mice were used to generate *ErbB4*<sup>Flox</sup>/*Pax8-Cre* mice. CD-1 mice were used to examine *ErbB4* expression in wild-type embryos and newborn mice (Figure 1),



whereas all the mutant mice were maintained and bred in C57BL/6 background.

### Real-Time RT-PCR

Real-time RT-PCR was carried out using primers and probes listed in Supplemental Table 1 or described earlier.<sup>38</sup>

### In Situ Hybridization

*In situ* hybridization analysis of *ErbB4* expression was carried out at Max Planck Institute of Biophysical Chemistry (Gene Paint database; <http://www.genepaint.org>). *Slc3A1* expression was analyzed as described elsewhere.<sup>39</sup>

### Immunostaining

Proliferation was assessed from paraffin-embedded sections using a PCNA staining kit (Invitrogen, Carlsbad, CA). ErbB4 immunohistochemistry was carried out, as described elsewhere,<sup>38</sup> except that sc-283 (Santa Cruz Biotechnology, Santa Cruz, CA) was used as the primary antibody. HIF-1 $\alpha$  immunohistochemistry was done with H1 $\alpha$ 67 (Abcam, Cambridge, UK) primary antibody using Histo-Mouse-MAX kit (Invitrogen). To identify fibrotic tissue, paraffin sections were stained with Masson trichrome.<sup>40</sup>

Immunofluorescence staining of paraffin sections was carried out using primary antibodies against aquaporin-1 (Millipore, Billerica, MA), aquaporin-2 (Sigma-Aldrich, St. Louis, MO), thiazide-sensitive NaCl cotransporter (Millipore), phospho-histone H3 (Millipore), acetylated  $\alpha$ -tubulin (Sigma-Aldrich), DBA (rhodamine labeled) (Vector Laboratories, Burlingame, CA), *Lotus tetragonolobus* lectin (fluorescein labeled) (Vector Laboratories), anti-ZO-1 (Invitrogen), or E-cadherin (BD Biosciences, Franklin Lakes, NJ), and Alexa Fluor 488- or 546-conjugated secondary antibodies (Invitrogen). Nuclei were stained with 4',6-diamidino-2-phenylindole (Sigma Pharmaceuticals).

Immunofluorescence staining of MDCK cells was carried out, as described elsewhere,<sup>14</sup> using the following primary antibodies: anti-E-cadherin (rrl),<sup>41</sup> anti-podocalyxin (gp135),<sup>42</sup> anti-ZO-1 (Invitrogen), and anti-Ki-67 (Invitrogen). Anti-podocalyxin and anti-E-cadherin were gifts from Dr. Kai Simons (MPI-CBG, Dresden, Germany). The primary antibodies were detected using Alexa Fluor 488- or 546-conjugated secondary antibodies and the nuclei were stained with 4',6-diamidino-2-phenylindole.

To evaluate the orientation of cell division, sections of newborn *R26ERBB4/Pax8-Cre* mouse kidneys were immunostained with anti-phospho-histone H3 and anti-E-cadherin antibodies.

### Western Blotting

Proteins were extracted from MDCK cells or embryonic and newborn kidneys and analyzed by Western blotting using anti-ErbB4 (E200) (Abcam), anti-phospho-ErbB4 (#4757; Cell Signaling, Danvers, MA), anti-Akt (sc-1618; Santa Cruz Biotechnology), anti-phospho-Akt (#9271; Cell Signaling), anti-Erk (#9102; Cell Signaling), anti-phospho-Erk (#9101; Cell Signaling), anti- $\beta$ -actin (sc-1616; Santa Cruz Biotechnology), and anti-glyceraldehyde 3-phosphate dehydrogenase (Millipore) antibodies, as described elsewhere.<sup>43</sup>

### Three-Dimensional Culture of MDCK Cells

MDCK cells were transduced with retroviral constructs encoding *ERBB4 JM-a CYT-2* (pBABE-puro*ErbB4JM-aCYT-2*) or an empty vector.<sup>44</sup> The transduced cells were cultured for 5 days in Matrigel and fixed with 4% paraformaldehyde.<sup>45</sup>

### Tissue Culture

For kidney mesenchyme tubule induction assays, E11.5 mesenchymes were separated from the ureteric buds and cultured for 0, 48, 96, or 120 hours in combination with a heterologous tubule inducer tissue, a dorsal piece of E11.5 embryonic spinal cord.<sup>46</sup>

### Targeting of Human *ERBB4* cDNA into the *Rosa26* Locus to Generate a Mouse Model for Conditional Expression

Human *ERBB4 JM-a CYT-2* cDNA was amplified by PCR (Supplemental Table 2, PCR I) from a vector pcDNA3.1*ErbB4JM-aCYT-2*.<sup>11</sup> The amplified PCR fragment was cloned into a pRosa26-DEST vector.<sup>47</sup> This generated a targeting vector, pRosa26-DEST-*ERBB4*, that contained the *ERBB4* insert under a floxed transcriptional stop cassette. The targeting vector was electroporated into a SV-129 mouse embryonic stem cells. Targeting to the *Rosa26* locus (Supplemental Figure 1A) was identified by Southern blotting<sup>48</sup> and by PCR (Supplemental Table 2, PCR II; Supplemental Figure 1B) and was confirmed by sequencing.

Selected embryonic stem cells were injected into blastocyst stage C57BL/6 mouse embryos to obtain chimeras. The chimeric mice were screened for germline transmission to obtain F<sub>1</sub> progeny of the *R26ERBB4*<sup>+/-</sup> mice that were heterozygous for the *ERBB4 JM-a CYT-2* cDNA under a floxed transcriptional stop cassette inserted to the *Rosa26* locus. The F<sub>1</sub> mice were bred with C57BL/6 mice to produce F<sub>2</sub> progeny. The heterozygous *R26ERBB4*<sup>+/-</sup> mice were further crossed with the *Pax8-Cre* recombinase-positive mice<sup>15</sup> to obtain *R26ERBB4/Pax8-Cre* mice (Supplemental Figure 2).

### Statistical Analyses

A *t* test was used to statistically analyze morphometric and immunohistochemical data. A chi-squared test was used to determine whether the number of *ErbB4*<sup>Flox/Flox</sup>/*Pax8-Cre*<sup>+</sup> pups and embryos deviated from the expected Mendelian ratios. The statistical analyses were done using the SPSS Statistics program (Version 19.0.0; IBM, Armonk, NY).

### ACKNOWLEDGMENTS

We thank Hannele Härkman, Johanna Kekolahti-Liias, Jaana Kujala, Merja Lakkisto, and Tuula Oivanen for excellent technical assistance. We also thank Ilkka Paatero for assistance with HIF immunohistochemistry and Ana Martinez-Hernandez at the Max Planck Institute of Biophysical Chemistry for help with the *ErbB4 in situ* hybridization.

This work was supported by the Academy of Finland, European Union, Finnish Cancer Organizations, Foundation for the Finnish Cancer Institute, Sigrid Jusélius Foundation, and Turku University Foundation.

## DISCLOSURES

None.

## REFERENCES

- Yarden Y, Sliwkowski MX: Untangling the ErbB signalling network. *Nat Rev Mol Cell Biol* 2: 127–137, 2001
- Gassmann M, Casagrande F, Orioli D, Simon H, Lai C, Klein R, Lemke G: Aberrant neural and cardiac development in mice lacking the ErbB4 neuregulin receptor. *Nature* 378: 390–394, 1995
- Tidcombe H, Jackson-Fisher A, Mathers K, Stern DF, Gassmann M, Golding JP: Neural and mammary gland defects in ErbB4 knockout mice genetically rescued from embryonic lethality. *Proc Natl Acad Sci USA* 100: 8281–8286, 2003
- Srinivasan R, Poulsom R, Hurst HC, Gullick WJ: Expression of the c-erbB-4/HER4 protein and mRNA in normal human fetal and adult tissues and in a survey of nine solid tumour types. *J Pathol* 185: 236–245, 1998
- Zeng F, Zhang MZ, Singh AB, Zent R, Harris RC: ErbB4 isoforms selectively regulate growth factor induced Madin-Darby canine kidney cell tubulogenesis. *Mol Biol Cell* 18: 4446–4456, 2007
- Thomasson M, Hedman H, Junttila TT, Elenius K, Ljungberg B, Henriksson R: ErbB4 is downregulated in renal cell carcinoma—a quantitative RT-PCR and immunohistochemical analysis of the epidermal growth factor receptor family. *Acta Oncol* 43: 453–459, 2004
- Nemo R, Murcia N, Dell KM: Transforming growth factor alpha (TGF- $\alpha$ ) and other targets of tumor necrosis factor- $\alpha$  converting enzyme (TACE) in murine polycystic kidney disease. *Pediatr Res* 57: 732–737, 2005
- Junttila TT, Sundvall M, Määttä JA, Elenius K: ErbB4 and its isoforms: selective regulation of growth factor responses by naturally occurring receptor variants. *Trends Cardiovasc Med* 10: 304–310, 2000
- Sundvall M, Korhonen A, Paatero I, Gaudio E, Melino G, Croce CM, Aqeilan RI, Elenius K: Isoform-specific monoubiquitination, endocytosis, and degradation of alternatively spliced ErbB4 isoforms. *Proc Natl Acad Sci USA* 105: 4162–4167, 2008
- Ni CY, Murphy MP, Golde TE, Carpenter G: gamma-Secretase cleavage and nuclear localization of ErbB-4 receptor tyrosine kinase. *Science* 294: 2179–2181, 2001
- Määttä JA, Sundvall M, Junttila TT, Peri L, Laine VJ, Isola J, Egeblad M, Elenius K: Proteolytic cleavage and phosphorylation of a tumor-associated ErbB4 isoform promote ligand-independent survival and cancer cell growth. *Mol Biol Cell* 17: 67–79, 2006
- Sardi SP, Murtie J, Koirala S, Patten BA, Corfas G: Presenilin-dependent ErbB4 nuclear signaling regulates the timing of astrogenesis in the developing brain. *Cell* 127: 185–197, 2006
- O'Brien LE, Zegers MM, Mostov KE: Opinion: Building epithelial architecture: insights from three-dimensional culture models. *Nat Rev Mol Cell Biol* 3: 531–537, 2002
- Torkko JM, Manninen A, Schuck S, Simons K: Depletion of apical transport proteins perturbs epithelial cyst formation and ciliogenesis. *J Cell Sci* 121: 1193–1203, 2008
- Bouchard M, Souabni A, Busslinger M: Tissue-specific expression of cre recombinase from the Pax8 locus. *Genesis* 38: 105–109, 2004
- Devuyst O, Burrow CR, Smith BL, Agre P, Knepper MA, Wilson PD: Expression of aquaporins-1 and -2 during nephrogenesis and in autosomal dominant polycystic kidney disease. *Am J Physiol* 271: F169–F183, 1996
- Karner CM, Chirumamilla R, Aoki S, Igarashi P, Wallingford JB, Carroll TJ: Wnt9b signaling regulates planar cell polarity and kidney tubule morphogenesis. *Nat Genet* 41: 793–799, 2009
- Pazour GJ, San Agustin JT, Folliot JA, Rosenbaum JL, Witman GB: Polycystin-2 localizes to kidney cilia and the ciliary level is elevated in orpk mice with polycystic kidney disease. *Current Biology* 12:R378.
- Schmitt R, Ellison DH, Farman N, Rossier BC, Reilly RF, Reeves WB, Oberbäumer I, Tapp R, Bachmann S: Developmental expression of sodium entry pathways in rat nephron. *Am J Physiol* 276: F367–F381, 1999
- Fischer E, Legue E, Doyen A, Nato F, Nicolas JF, Torres V, Yaniv M, Pontoglio M: Defective planar cell polarity in polycystic kidney disease. *Nat Genet* 38: 21–23, 2006
- Yu J, Carroll TJ, Rajagopal J, Kobayashi A, Ren Q, McMahon APA: A Wnt7b-dependent pathway regulates the orientation of epithelial cell division and establishes the cortico-medullary axis of the mammalian kidney. *Development* 136: 161–171, 2009
- Yang D, Lai D, Huang X, Shi X, Gao Z, Huang F, Zhou X, Geng YJ, et al: The defects in development and apoptosis of cardiomyocytes in mice lacking the transcriptional factor Pax-8. [published online ahead of print September 17, 2010] *Int J Cardiol*. 10.1016/j.ijcard.2010.08.057
- Elenius K, Corfas G, Paul S, Choi CJ, Rio C, Plowman GD, Klagsbrun M: A novel juxtamembrane domain isoform of HER4/ErbB4. Isoform-specific tissue distribution and differential processing in response to phorbol ester. *J Biol Chem* 272: 26761–26768, 1997
- Sundvall M, Veikkolainen V, Kurppa K, Salah Z, Tvorogov D, van Zoelen EJ, Ageilan R, Elenius K, et al: Cell death or survival promoted by alternative isoforms of ErbB4. *Mol Biol Cell* 21:4275–4286, 2010.
- Muraoka-Cook RS, Sandahl MA, Strunk KE, Miraglia LC, Husted C, Hunter DM, Elenius K, Chodosh LA, Earp HS 3rd: ErbB4 splice variants Cyt1 and Cyt2 differ by 16 amino acids and exert opposing effects on the mammary epithelium in vivo. *Mol Cell Biol* 29: 4935–4948, 2009
- Takata K, Matsuzaki T, Tajika Y, Ablimit A, Hasegawa T: Localization and trafficking of aquaporin 2 in the kidney. *Histochem Cell Biol* 130: 197–209, 2008
- Saburi S, Hester I, Fischer E, Pontoglio M, Eremina V, Gessler M, Quaggin SE, Harrison R, Mount R, McNeill H: Loss of Fat4 disrupts PCP signaling and oriented cell division and leads to cystic kidney disease. *Nat Genet* 40: 1010–1015, 2008
- Veland IR, Awan A, Pedersen LB, Yoder BK, Christensen ST: Primary cilia and signaling pathways in mammalian development, health and disease. *Nephron, Physiol* 111: 39, 2009
- Backx L, Ceulemans B, Vermeesch JR, Devriendt K, Van Esch H: Early myoclonic encephalopathy caused by a disruption of the neuregulin-1 receptor ErbB4. *Eur J Hum Genet* 17: 378–382, 2009
- Sweeney WE Jr, Avner ED: Functional activity of epidermal growth factor receptors in autosomal recessive polycystic kidney disease. *Am J Physiol* 275: F387–F394, 1998
- Nakanishi K, Sweeney W Jr, Avner ED: Segment-specific c-ErbB2 expression in human autosomal recessive polycystic kidney disease. *J Am Soc Nephrol* 12: 379–384, 2001
- Wilson PD, Du J, Norman JT: Autocrine, endocrine and paracrine regulation of growth abnormalities in autosomal dominant polycystic kidney disease. *Eur J Cell Biol* 61: 131–138, 1993
- Du J, Wilson PD: Abnormal polarization of EGF receptors and autocrine stimulation of cyst epithelial growth in human ADPKD. *Am J Physiol* 269: C487–C495, 1995
- Wilson SJ, Amsler K, Hyink DP, Li X, Lu W, Zhou J, Burrow CR, Wilson PD: Inhibition of HER-2(neu/ErbB2) restores normal function and structure to polycystic kidney disease (PKD) epithelia. *Biochim Biophys Acta* 1762: 647–655, 2006.
- Sweeney WE Jr, von Vigier RO, Frost P, Avner ED: Src inhibition ameliorates polycystic kidney disease. *J Am Soc Nephrol* 19: 1331–1341, 2008
- Long W, Wagner KU, Lloyd KC, Binart N, Shillingford JM, Hennighausen L, Jones FE: Impaired differentiation and lactational failure of ErbB4-deficient mammary glands identify ERBB4 as an obligate mediator of STAT5. *Development* 130: 5257–5268, 2003
- Jokela T, Vainio S: Conditional tamoxifen Cre induced mutagenesis in the embryonic kidney in organ culture. *Genesis* 45: 757–761, 2007
- Junttila TT, Laato M, Vahlberg T, Söderström KO, Visakorpi T, Isola J, Elenius K: Identification of patients with transitional cell carcinoma of

- the bladder overexpressing ErbB2, ErbB3, or specific ErbB4 isoforms: Real-time reverse transcription-PCR analysis in estimation of ErbB receptor status from cancer patients. *Clin Cancer Res* 9: 5346–5357, 2003
39. Zhang S, Lin Y, Itäranta P, Yagi A, Vainio S: Expression of Sprouty genes 1, 2 and 4 during mouse organogenesis. *Mech Dev* 109: 367–370, 2001
  40. Sheehan DC, Hrapchak BB: *Theory and Practice of Histotechnology*, St. Louis, London, Mosby, 1980
  41. Gumbiner B, Simons K: A functional assay for proteins involved in establishing an epithelial occluding barrier: Identification of a uvomorulin-like polypeptide. *J Cell Biol* 102: 457–468, 1986
  42. Ojakian GK, Schwimmer R: The polarized distribution of an apical cell surface glycoprotein is maintained by interactions with the cytoskeleton of Madin-Darby canine kidney cells. *J Cell Biol* 107: 2377–2387, 1988
  43. Kainulainen V, Sundvall M, Määttä JA, Santiestevan E, Klagsbrun M, Elenius K: A natural ErbB4 isoform that does not activate phosphoinositide 3-kinase mediates proliferation but not survival or chemotaxis. *J Biol Chem* 275: 8641–8649, 2000
  44. Tvorogov D, Sundvall M, Kurppa K, Holmén M, Repo S, Johnson MS, Elenius K: Somatic mutations of ErbB4: selective loss-of-function phenotype affecting signal transduction pathways in cancer. *J Biol Chem* 284: 5582–5591, 2009
  45. Friedrichs J, Torkko JM, Helenius J, Teräväinen TP, Füllekrug J, Muller DJ, Simons K, Manninen A: Contributions of galectin-3 and -9 to epithelial cell adhesion analyzed by single cell force spectroscopy. *J Biol Chem* 282: 29375–29383, 2007
  46. Kispert A, Vainio S, Shen L, Rowitch DH, McMahon AP: Proteoglycans are required for maintenance of Wnt-11 expression in the ureter tips. *Development* 122: 3627–3637, 1996
  47. Hohenstein P, Slight J, Ozdemir DD, Burn SF, Berry R, Hastie ND: High-efficiency Rosa26 knock-in vector construction for Cre-regulated overexpression and RNAi. *Pathogenetics* 1: 3, 2008
  48. Soriano P: Generalized lacZ expression with the ROSA26 Cre reporter strain. *Nat Genet* 21: 70–71, 1999
  49. Rio C, Buxbaum JD, Peschon JJ, Corfas G: Tumor necrosis factor- $\alpha$ -converting enzyme is required for cleavage of erbB4/HER4. *J Biol Chem* 275: 10379–10387, 2000

---

See related editorial, “Polarity and Renal Cystogenesis,” on pages 4–5.

This article contains supplemental material online at <http://jasn.asnjournals.org/lookup/suppl/doi:10.1681/ASN.2011020160/-/DCSupplemental>.